

Effect of Polypropylene Fiber Reinforced Cement Composites for Enhancing the Seismic Performance of a Full-Scale Bridge Column Based on E-Defense Excitation



R.G. Zafra

Department of Civil Engineering, University of the Philippines Los Baños, Philippines

K. Kawashima

Department of Civil Engineering, Tokyo Institute of Technology, Japan

T. Sasaki, K. Kajiwara & M. Nakayama

Hyogo Earthquake Engineering Research Center, National Research Institute for Earth Science and Disaster Prevention, Japan

SUMMARY:

The effect of polypropylene fiber reinforced cement composites (PFRC) for enhancing the seismic performance of a full-scale bridge column is investigated. PFRC was incorporated at the plastic hinge region and part of the footing. Using the E-Defense shake-table, the column was subjected to three components of the near-field ground motion recorded at the JR Takatori station during the 1995 Kobe, Japan earthquake. Excitations were repeated under increased mass and increased intensity of ground motion. After six times of excitation, experimental results showed that use of PFRC substantially mitigated cover concrete damage and local buckling of longitudinal bars. Measured strains of tie reinforcements at the plastic hinge were also smaller. Moreover, there was no visible damage in the core concrete at the plastic hinge after the series of excitations. The damage sustained by the column using PFRC was much less than the damage of regular reinforced concrete columns.

Keywords: Polypropylene fiber reinforced cement composites; bridge column; shake-table experiments

1. INTRODUCTION

Bridges are vital components of transportation networks and they are vulnerable to seismic effects. Damage of bridges extensively occurred in past earthquakes such as the 1989 Loma Prieta, USA earthquake, 1994 Northridge, USA earthquake, 1995 Kobe, Japan earthquake, 1999 Chi Chi, Taiwan earthquake, 2008 Wenchuan, China earthquake, 2010 Maule, Chile earthquake and recently the 2011 East Japan earthquake. Thus, it is of utmost importance to insure the functionality of bridges even under significant earthquakes.

To investigate the seismic response of bridges, a large-scale bridge experimental program was conducted in 2007-2010 by the National Research Institute for Earth Science and Disaster Prevention (NIED), Japan (Nakashima et al., 2008). In the program, shake table experiments were conducted for two typical reinforced concrete columns which failed during the 1995 Kobe, Japan earthquake (C1-1 and C1-2 experiments), a typical reinforced concrete column designed in accordance with the 2002 Japan design code (JRA 2002) (C1-5 experiment) and a new generation column using an innovative material, polypropylene fiber reinforced cement composites (PFRC), for enhancing the damage control and ductility (C1-6 experiment) (Kawashima et al., 2012).

PFRC is a type of engineered cementitious composites (ECC) belonging to the class of high performance fiber reinforced cement composites (HPFRCC) (Hirata et al., 2009). ECCs have tensile strain capacity of about 0.03 to 0.05 resulting from the formation of closely spaced micro cracks due to the bridging action of fibers (Li and Leung, 1992; Li and Lepech, 2005). They have low elastic stiffness compared to concrete due to the absence of coarse aggregates and larger strain at peak compressive strength (Kesner, Billington and Douglas, 2003).

At present, HPFRCCs are used in the plastic hinge region of flexural members such as beams,

columns, structural wall bases, and in members with shear-dominated response such as beam-column connections, squat walls and coupling beams (Li, 1998; Parra-Montesinos, 2005). Recent applications include the use of ECC with polyvinyl alcohol (PVA) fibers in one of the bents of a 1/4-scale, four-span bridge model subjected to shake-table excitations (Cruz and Saiidi, 2012). HPRCCs have also been used for seismic retrofit applications such as dampers (Fukuyama and Suwada, 2003), infill panel walls (Kesner and Billington, 2005) and concrete jacket (Kosa et al., 2007). The deformation capacity and energy absorption capacity of structural members were significantly improved (Matsumoto and Mihashi, 2003).

Prior to the C1-6 experiment, bilateral cyclic loading experiments were conducted on 1.68 m high, 0.4 m by 0.4 m square cantilever reinforced concrete (RC) column and a column each using steel fiber reinforced concrete (SFRC) and PFRC at the plastic hinge region and the footing for deciding the material of C1-6 column (Kawashima et al., 2011). The column using PFRC had superior performance compared to the RC and SFRC columns due to the substantial mitigation of cover and core concrete damage, mitigation of longitudinal bar buckling and deformation of tie bars at the plastic hinge region. The current study investigates the effect of PFRC for enhancing the damage control and ductility capacity of a full-scale bridge column subjected to a near-field ground motion based on shake table experiments.

2. E-DEFENSE SHAKE-TABLE EXCITATIONS

2.1. Column configuration and properties

Fig. 1 shows C1-6 column which is a 7.5 m tall, 1.8 m by 1.8 m square, cantilever column. It was designed based on the 2002 Japan Specifications for Highway Bridges assuming moderate soil condition under the Type II design ground motion (near-field ground motion). PFRC was used at a part of the column with a depth of 2.7 m above the column base and a part of the footing with a depth of 0.60 m below the column base to minimize the volume of PFRC. The 2.7 m depth of PFRC is three times the estimated plastic hinge length of one-half the column width (JRA 2002) corresponding to 0.9 m to avoid failure at the PFRC-concrete interface. The 0.6 m depth of PFRC at the footing was decided to minimize damage. Regular concrete with design compressive strength of 30 MPa was used in the other parts of the column. The 2.7 m depth at the column and 0.6 m depth at the footing may be reduced after careful examination of damage at the PFRC-concrete interface.

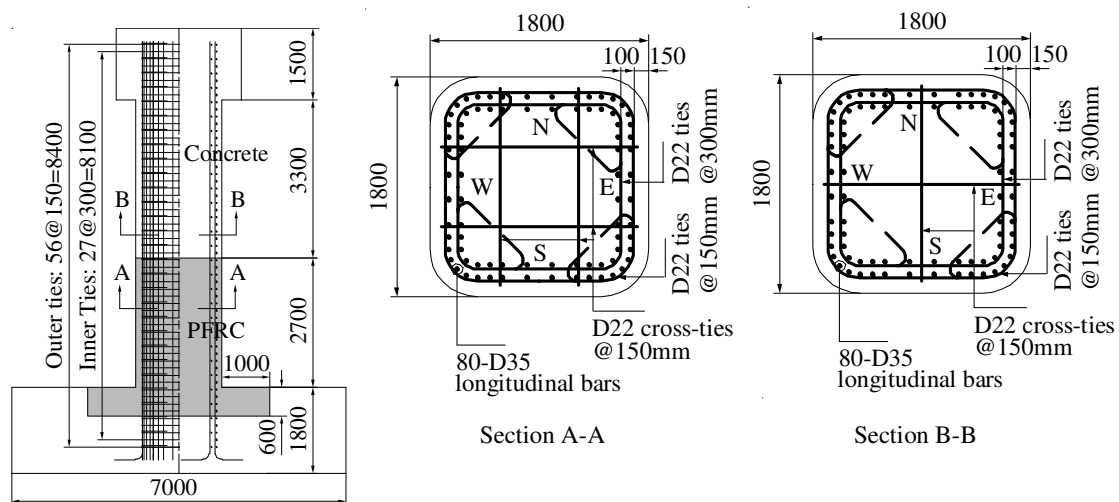


Figure 1. C1-6 column configuration and dimensions (mm)

The design compressive strength of PFRC was 40 MPa. PFRC was made by combining cement mortar, fine aggregates with maximum grain size of 0.30 mm, water and 3% volume of polypropylene fibers. Fibrillated polypropylene fibers with diameter of 42.6 μm , length of 12 mm, tensile strength of 482 MPa, Young's modulus of 5 GPa and density of 0.91 kg/m^3 were used (Hirata et al. 2009). Superplasticizers were added to improve the workability of the mix.

The longitudinal and tie bars had nominal yield strength of 345 MPa (SD345). Eighty-35 mm diameter deformed longitudinal bars were provided in two layers corresponding to a reinforcement ratio ρ_l of 2.47%. Deformed 22 mm diameter ties with 135 degree bent hooks lap spliced with 40 times the bar diameter were provided. Outer ties were spaced at 150 mm and inner ties were spaced at 300 mm throughout the column height. Cross-ties with 180 degree hooks at 150 mm spacing were provided to increase the confinement of the square ties. Volumetric tie reinforcement ratio ρ_s within a height of 2.7 m from the column base was 1.72%. Concrete cover of 150 mm was provided.

2.2. Experiment set-up and shake-table excitations

Photo 1 shows the experiment set-up using the E-Defense shake table. Four mass blocks were set on the column through two simply supported decks. The decks were used to fix the mass blocks to the column but were not designed to idealize the stiffness and strength of real decks. Each deck was supported by the column on one side and by the steel end support on the other side.

A 78 tf (765 kN) mass block and a 45 tf (441 kN) mass block were fixed to each deck as close to the column as possible so that tributary weight in the transverse direction could be maximum. The total weight consisting of four mass blocks, two decks, two fixed bearings, two movable bearings, eight side sliders and 32 load cells was 307 tf (3012 kN). Note that the tributary weight which generated the inertia force in the column in the transverse direction was 215 tf (2109 kN), about 2/3 of the total weight. The total weight of the entire experiment set-up including the column and the two end-supports was 1069 tf (10.5 MN), which was close to the payload of 1200 tf (12 MN).



Photo 1. Experiment set-up using E-Defense shake table

The column was excited using the near-field ground motion recorded at the JR Takatori Station during the 1995 Kobe earthquake. Although duration was short, it was one of the most destructive ground motions to structures with peak ground acceleration (PGA) of 0.62g and peak ground velocity (PGV) of 1.19 m/s in the fault-normal direction (JRTRI 1999). Because the energy dissipation of a column anchored to a shake table is extremely less than the real energy dissipation of a column embedded in the ground (Sakai and Unjoh, 2006), a ground motion with 80% of the original intensity of the JR Takatori record was imposed as a command to the table in the experiment to take into account the effect of soil-structure interaction. This ground motion is called the 100% E-Takatori ground motion. Fig. 2 shows the EW, NS and UD components of the 100% E-Takatori ground motion which were applied in the longitudinal, transverse and vertical directions, respectively, of the bridge model. The corresponding acceleration response spectra at 5% damping is also shown.

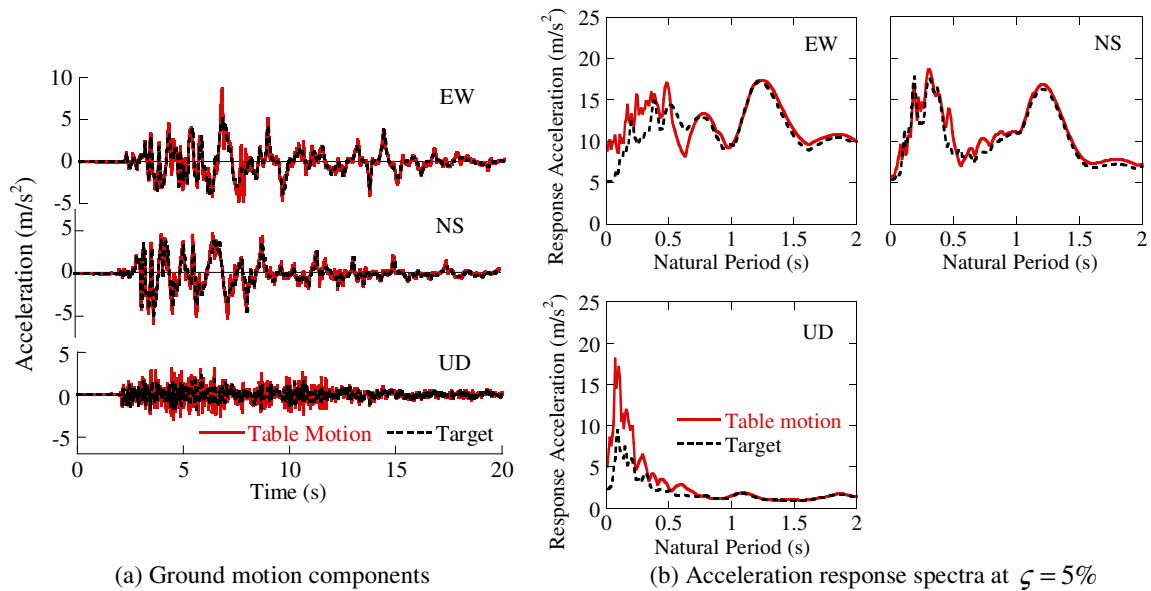


Figure 2. E-Takatori ground motion

Shake table excitations were conducted six times. Excitations were repeated to clarify column performance when subjected to much stronger and longer duration near-field ground motion. The column was excited twice with 100% E-Takatori ground motion (1-100%(1) and 1-100%(2) excitations). After the mass in the longitudinal direction was increased by 21% from 307 tf to 372 tf, excitations were conducted with 100% E-Takatori ground motion once (2-100% excitation) and 125% E-Takatori ground motion three times (2-125%(1), 2-125%(2) and 2-125%(3) excitations).

3. COLUMN SEISMIC PERFORMANCE

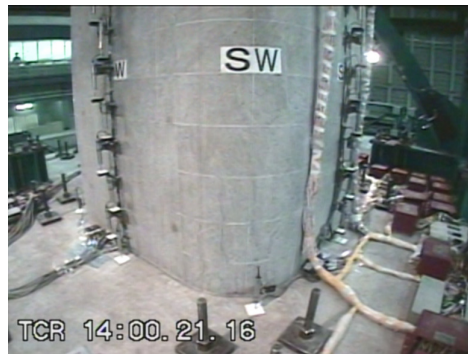
3.1. Damage progress

Photos 2 to 4 show the damage progress within 1.2 m from the column base at the SW and NE corners during 1-100%(1), 2-100% and 2-125%(3) excitations at the instance of peak response displacement where the SW corner was subjected to the largest compression while the NE corner was subjected to the largest tension during the excitations. As shown in Photo 2, during 1-100%(1) excitation, only micro cracks were observed around the column. Although photograph during 1-100%(2) excitation is not shown here, very thin flexural cracks as wide as 0.1 - 0.2 mm occurred within 1.6 m from the base all around the column.

During 2-100% excitation, with the mass increased by 21%, damage progressed as shown in Photo 3. Flexural cracks propagated and a crack 0.6 m from the column base at the NE corner opened about 8 mm at the peak response displacement occurring at 6.78 s. After the excitation, the maximum residual crack at the above location was 1 - 2 mm wide. Although only flexural cracks occurred all around the column with the cover concrete remaining as a whole shell due to the bridging action of fibers, vertical hairline cracks started to occur at the NE and SW corners within 0.6 m from the column base due to the large strut action of cover concrete shell resulting from the footing reaction when the column was laterally displaced.

During 2-125%(1) excitation, in which the seismic excitation intensity was increased by 25%, at the peak response displacement at 6.97 s, the crack 0.6 m from the base opened to 14 mm at the NE corner which was subjected to tension while a vertical crack opened to 9 mm at the opposite SW corner subjected to compression. As the loading progressed, at the SW corner subjected to tension, a crack

1.2 m from the base opened to 9 mm and vertical cracks started to widen at the opposite NE corner. Succeeding excitations resulted to further propagation of flexural cracks within 2 m from the base around the column and the widening of the vertical crack at the SW corner. As shown in Photo 4, the damage progressed during 2-125%(3) excitation wherein at the peak response displacement at 7.07 s, the crack 0.6 m from the base at the NE corner opened to 20 mm and the vertical crack at the SW corner opened to 15 mm. Note that at the NW corner, cover concrete spalled within 200 mm from the column base when it was subjected to compression while flexural cracks opened to 13 mm at the opposite SE corner subjected to tension. After the excitation, the cracks which opened to over 10 mm during the excitation almost closed with widths of only 5 - 8 mm in flexural cracks and 7 - 12 mm in vertical cracks. Moreover, majority of other small cracks closed to hairline cracks after the excitations due to the bridging action of fibers. Cover concrete spalling was much restricted and there were no exposed longitudinal bars and ties in C1-6 column after 2-125%(3) excitation.



(a) SW corner



(b) NE corner

Photo 2. Column damage during 1-100%(1) excitation



(a) SW corner



(b) NE corner

Photo 3. Column damage during 2-100% excitation



(a) SW corner



(b) NE corner

Photo 4. Column damage during 2-125%(3) excitation

To investigate how damage progressed in the core and the longitudinal bars after the last excitation, cover concrete was removed at the SW and NE corners using an electric drill and saw. Removal of cover concrete in the fiber mixed concrete was difficult due to the presence of fibers compared to that of regular reinforced concrete. Photo 5(a) shows the opened area at the NE corner after the outer ties were removed to facilitate inspection of the outer and inner longitudinal bars for local buckling. Three outer longitudinal bars buckled in between outer ties at 250 mm and 550 mm from the base. Note that ties at these locations have double tie area because of the 40 times bar lap splice and development of the 135 degree hook. Since confinement was higher at these locations, bar buckling did not occur at these locations. The maximum lateral offset among the three longitudinal bars from their original vertical axis was 8 mm. On the other hand, the inner longitudinal bars did not buckle because they were constrained by the undamaged concrete between the outer and inner longitudinal bars.

Photo 5(c) shows that at the location where a crack opened to 20 mm, the crack occurred only in the cover concrete with a depth of 110 mm and did not propagate into the core concrete. Photo 5(d) shows the block of cover concrete that was removed at the bottom right portion of the NE corner where the presence of fibers held the cover concrete together preventing the disintegration of cover concrete. Hence, it is worthy to note that even after six times of excitation, the damage sustained by C1-6 column was much less than the damage of regular reinforced concrete columns.

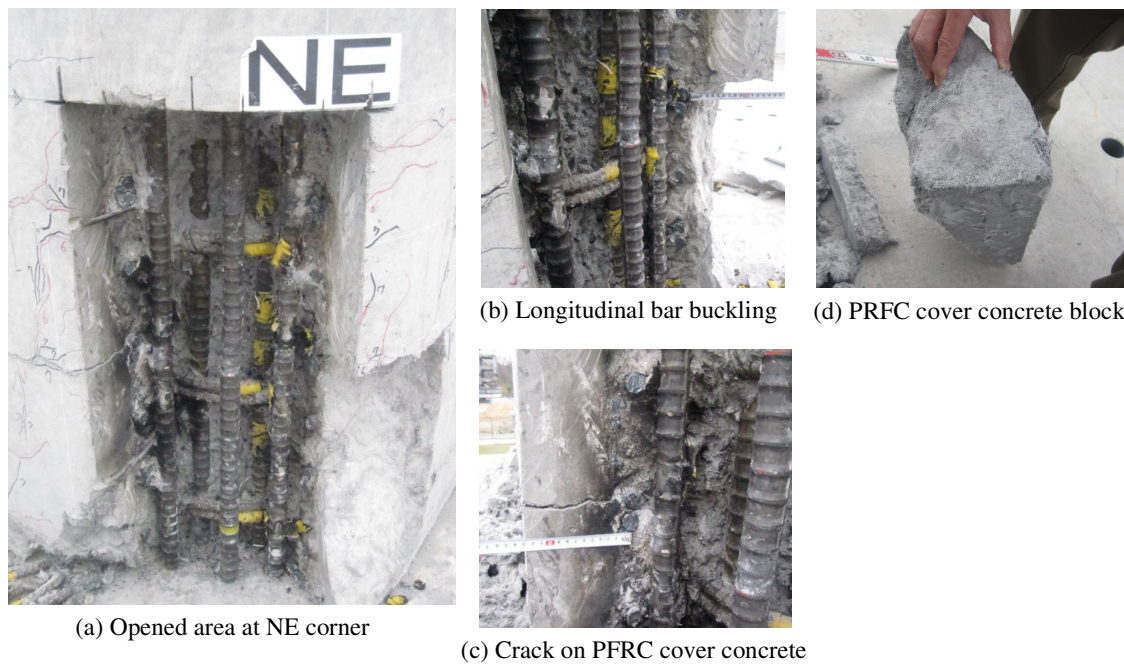


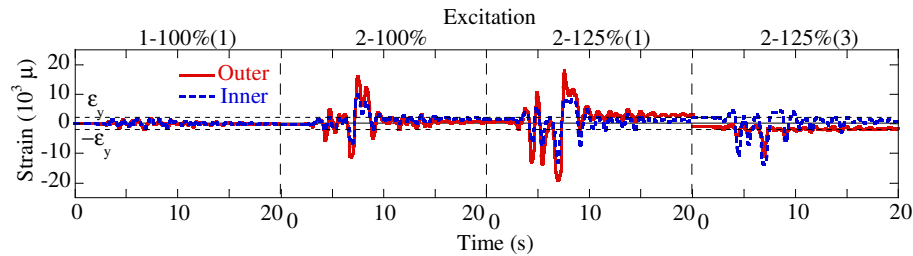
Photo 5. Damage of PFRC cover concrete and longitudinal bars at the NE corner after 2-125%(3) excitation

3.2 Strains of longitudinal and tie bars

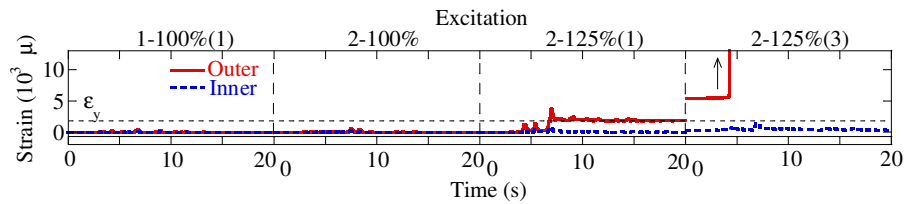
Fig. 3 shows the strains of longitudinal and tie bars of C1-6 column at the plastic hinge zone (300-400 mm from the base) at the SW corner where the most extensive damage occurred. Only strains during 1-100%(1), 2-100%, 2-125%(1) and 2-125%(3) excitations are shown due to space limitation. Because longitudinal bars were set in two layers, strains of both the outer and inner longitudinal bars and tie bars are shown here. Noting that the yield strain of both longitudinal and tie bars was nearly $2,000 \mu$, the longitudinal bars started to yield in tension during 1-100%(1) while tie bars started to yield in tension during 2-125%(1) excitation. The outer and inner longitudinal bars and tie bars exhibited similar response however the amplitude of strains were generally larger in the outer longitudinal and tie bars than the respective inner longitudinal and tie bars. The difference of strain amplitude between outer and inner tie bars is particularly large during and after 2-125%(1) excitation resulting from local buckling of longitudinal bars, which will be described later.

An interesting point in Fig. 3 is that the compression strains of the outer and inner longitudinal bars became larger than tension strains during and after 2-125%(1) excitation. For example, compression strain of the outer longitudinal bar reached $19,000\mu$ while tension strain reached $18,000\mu$ during 2-125%(1) excitation. This obviously resulted from the low elastic modulus of PFRC. The large compression strain must have caused the longitudinal bar to buckle. However, in spite of the bar buckling, as described in Section 3.1, spalling of cover concrete did not occur indicating that the presence of fibers made the cover concrete remain as a whole shell.

On the other hand, the tie bar was still elastic during 1-100%(1) until 2-100% excitations. At 6.97s, when compression strain of the outer longitudinal bar sharply increased during 2-125%(1) excitation, the outer tie strain started to increase to $3,700\mu$, indicating that the tie resisted the longitudinal bar buckling. Compression strain of the inner longitudinal bar also sharply increased at the same time, however, the inner tie strain did not increase indicating that the inner longitudinal bar did not buckle. This is because confinement for bar buckling was larger at the inner longitudinal bar than the outer longitudinal bar due to the resistance of core concrete between outer and inner ties which was still intact as shown in Photo 5.



(a) Longitudinal bars at 300 mm from the base



(b) Tie bars at 400 mm from the base

Figure 3. Strains of longitudinal bars and tie bars at the SW corner during 1-100%(1), 2-100%, 2-125%(1) and 2-125%(3) excitations

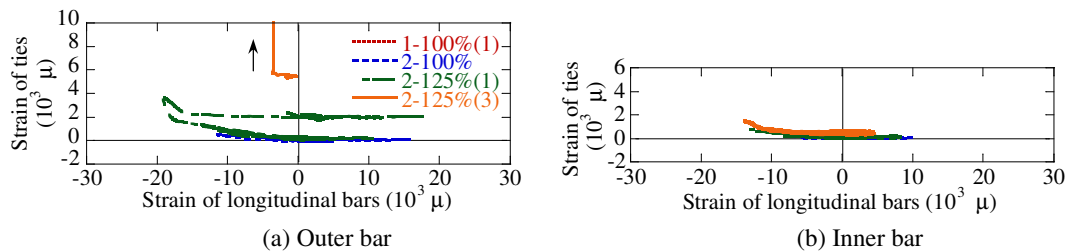


Figure 4. Strain of a tie at 400 mm from the base vs. strain of a longitudinal bar at 300 mm from the base at the SW corner

Fig. 4 shows the interaction of a longitudinal bar with a tie bar for outer and inner bars. The tie strains during 2-125%(3) excitation were larger than $5,000\mu$ and only reliable data are shown here. A sharp increase of the outer tie strain resulting from restraining local buckling of the outer longitudinal bar under high compression strain is clearly seen during and after 2-125%(1) excitation while the inner tie strain remained below $2,000\mu$ because inner longitudinal bars did not yet buckle.

3.3 Response acceleration and displacement

Fig. 5 shows the response acceleration and displacement at the top of column in the principal response direction and Table 1 summarizes the peak acceleration, displacement, residual displacement and moment at each excitation. The principal response direction is defined as the direction in which the response displacement was maximum. It is seen that the response acceleration has similar shape with the input ground acceleration at early excitations. However, in later excitations, the response acceleration tends to have almost uniform amplitude during the excitation, if several spikes with large amplitudes are eliminated, and this is due to the nonlinear response of the columns.

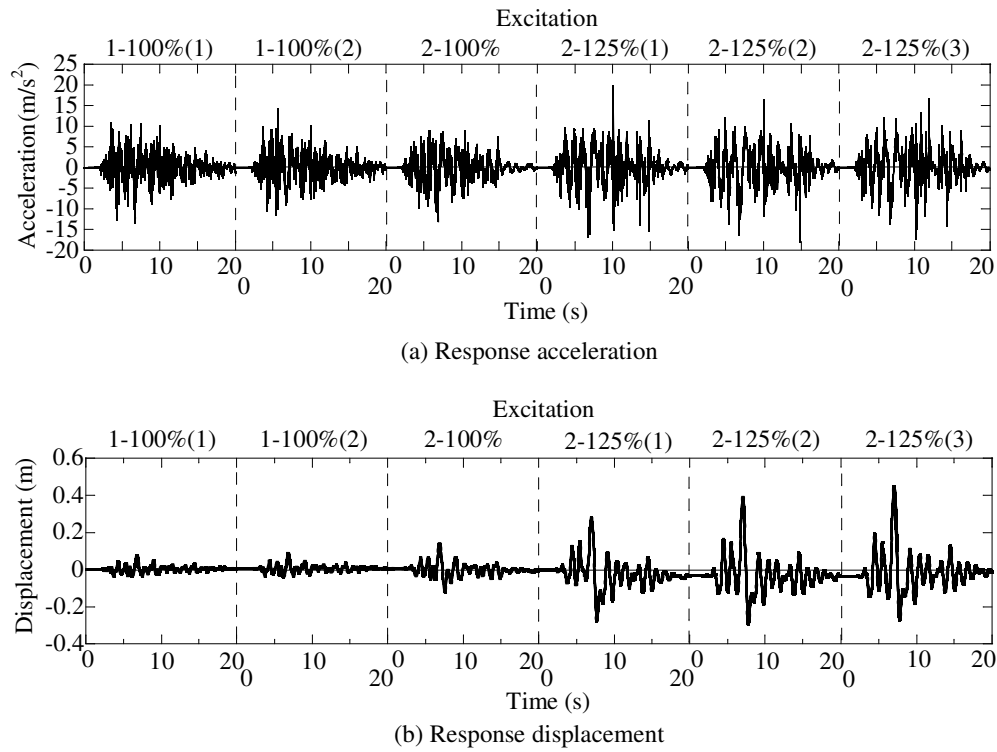


Figure 5. Column response in the principal direction

Table 1. Column response in the principal response direction

Excitation	Response Acceleration (m/s ²)	Response Displacement		Residual Displacement (m)	Moment (MNm)
		(m)	Drift (%)		
1-100%(1)	-13.4	0.078	1.0	0.005	20.5
1-100%(2)	14.2	0.089	1.2	0.007	21.8
2-100%	-13.0	0.144	1.9	-0.004	24.0
2-125%(1)	19.9	0.280	3.7	-0.035	24.3
2-125%(2)	-17.9	0.392	5.2	-0.037	25.3
2-125%(3)	-17.1	0.450	6.0	-0.013	24.9

Due to the high acceleration pulse in the input ground motion, the column experienced high amplitude displacement during each excitation. The peak response displacement was equal to 0.078 m (1.0% drift) during 1-100%(1) excitation and progressed to 0.45 m (6.0% drift) during 2-125%(3) excitation. As the excitation progressed with increasing mass and intensity of ground motion, the response displacements increased due to column stiffness deterioration resulting from the damage. Residual displacement was only -0.004 m (0.05% drift) after 2-100% excitation, increased to -0.037 m (0.49% drift) after 2-125%(2) excitation then decreased to -0.013 m (0.13% drift) after the last excitation. It is important to note that residual displacement not only increases but also decreases during seismic

excitations. Because instantaneous stiffness vary, instantaneous period also vary which causes changes in the residual displacement (MacRae and Kawashima, 1997). Since the allowable residual drift for a cantilever column based on the 2002 JRA code is 1%, the residual drift of the column was still smaller than the allowable limit.

3.4 Moment and ductility capacity

Fig. 6 shows the hysteresis of moment at the base vs. displacement at the top of the column in the principal response direction. The hysteresis during the entire six times of excitation is stable with sufficient energy dissipation. As summarized in Table 1, the peak moment gradually increased as the excitation progressed. A maximum capacity of 25.3 MNm at 5.2% drift was developed during 2-125%(2) excitation. During this excitation, flexural cracks further propagated all around the column and the vertical cracks at the SW corner widened as described in Section 3.1. During the subsequent 2-125%(3) excitation, the peak drift increased to 6% while the peak moment slightly deteriorated by 2%. It should be noted that even during the 2-125%(3) excitation, the moment vs. lateral displacement hysteresis was still very stable.

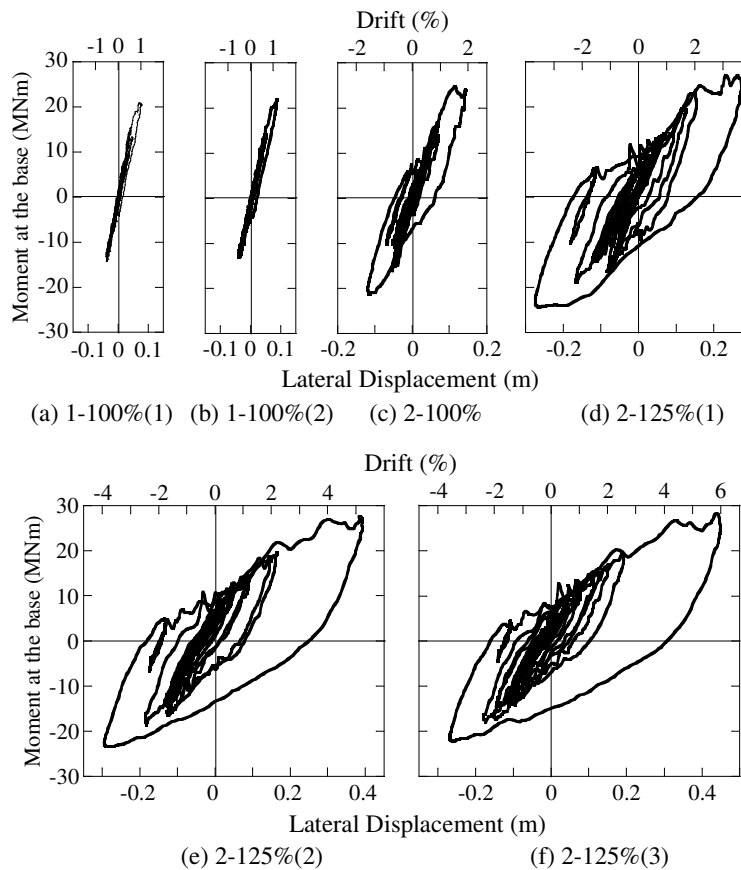


Figure 6. Hysteresis of moment at the base vs. displacement at the top of column in the principal direction

4. CONCLUSIONS

The seismic performance of a full-scale bridge column using polypropylene fiber reinforced cement composites (PFRC) subjected to near-field ground motions was investigated through shake table experiments. Based on the results presented, the following conclusions were obtained:

- a) Under a strong earthquake, the use of PFRC substantially reduced the apparent damage which can

- allow the bridge to be serviceable.
- b) PFRC did not have the brittle compression failure of regular reinforced concrete under repeated large inelastic deformation due to the bridging mechanism of fibers.
 - c) As a consequence of b), use of PFRC mitigated the buckling of outer longitudinal bars and the deformation of outer and inner tie bars. No visible buckling of inner longitudinal bars occurred due to the intact PFRC between outer and inner longitudinal bar layers.
 - d) Because the PFRC cover concrete of C1-6 column did not spall in a brittle manner compared to standard reinforced concrete columns, the cover concrete resisted the compression from the footing reaction at the base due to strut action as shell component, although vertical cracks occurred on the cover concrete.
 - e) As a result of the damage mitigation properties of PFRC, the column had a stable flexural capacity and enhanced ductility reaching until 6% drift.

REFERENCES

- Cruz, C. and Saiidi, M. (2012). Shake table studies of a 4-span bridge model with advanced materials. *Journal of Structural Engineering, ASCE* **138:2**, 183-192.
- Fukuyama, H. and Suwada, H. (2003). Experimental response of HPRC dampers for structural control. *Journal of Advanced Concrete Technology, JCI* **1:3**, 317-326.
- Japan Railway Technical Research Institute, West Japan Railway Company. (1999). JR Seismic Data, Kokubunji, Japan.
- Japan Road Association. (2002). Specifications for Highway Bridges, Maruzen, Tokyo.
- Hirata, T., Kawanishi, T., Okano, M. and Watanabe, S. (2009). Study on material properties and structural performance of high-performance cement composites using polypropylene fiber. *Proc. Japan Concrete Institute* **31:1**, 295-300.
- Kawashima, K., Zafra, R., Sasaki, T., Kajiwara, K. and Nakayama, M. (2011). Effect of polypropylene fiber reinforced cement composite and steel fiber reinforced concrete for enhancing the seismic performance of bridge columns. *Journal of Earthquake Engineering* **15:8**, 1194-1211.
- Kawashima, K., Zafra, R., Sasaki, T., Kajiwara, K., Nakayama, M., Unjoh, S., Sakai, J., Kosa, K., Takahashi, Y. and Yabe, M. (2012). Seismic performance of a full-size polypropylene fiber reinforced cement composite bridge column based on E-Defense shake-table experiments. *Journal of Earthquake Engineering* **16**.
- Kesner, K., Billington, S.L. and Douglas, K. (2003). Cyclic response of highly ductile fiber-reinforced cement-based composites. *ACI Materials Journal* **100:5**, 381-391.
- Kesner, K. and Billington, S. L. (2005). Investigation of infill panels made from engineered cementitious composites for seismic strengthening and retrofit. *Journal of Structural Engineering, ASCE* **131:11**, 1712-1720.
- Kosa, K., Wakita, K., Goda, H. and Ogawa, A. (2007) Seismic strengthening of piers with partial use of high ductility cement in *Advances in Construction Materials*, ed. C. U. Grosse (Springer, Berlin Heidelberg), 269-277.
- Li, V. (1998). Engineered cementitious composites (ECC) – tailored composites through micromechanical modeling in *Fiber Reinforced Concrete: Present and the Future*, eds. N. Banthia and A. Mufti (Canadian Society of Civil Engineers, Montreal, Canada), 64-97.
- Li, V. and Lepech, M. (2005) General design assumptions for engineered cementitious composites (ECC). *Proc. International RILEM Workshop on High Performance Fiber Reinforced Cementitious Composites (HPRC) in Structural Applications*, Hawaii, USA, 269-277.
- Li, V. and Leung, C. (1992). Steady-state and multiple cracking of short random fiber composites. *Journal of Engineering Mechanics, ASCE* **118:11**, 2246-2264.
- MacRae, G. and Kawashima, K. (1997). Post-earthquake residual displacements of bilinear oscillators. *Earthquake Engineering and Structural Dynamics* **26**, 701-716.
- Matsumoto, T. and Mihashi, H. (2003). DFRCC terminology and application concepts. *Journal of Advanced Concrete Technology, JCI* **1:3**, 335-340.
- Nakashima, M., Kawashima, K., Ukon, H. and Kajiwara, K.. (2008). Shake Table Experimental Project on the Seismic Performance of Bridges using E-Defense, *14th World Conference on Earthquake Engineering*, Beijing, China, Paper S17-02-010 (CD-ROM).
- Parra-Montesinos G. (2005). High-performance fiber-reinforced cement composites: an alternative for seismic design of structures. *ACI Structural Journal* **102:5**, 668-675.
- Saiidi, M. and Wang, H. (2006). Exploratory study of seismic response of concrete columns with shape memory alloys reinforcement. *ACI Structural Journal* **103:3**, 436-443.
- Sakai J and Unjoh S (2006). Earthquake simulation test of circular reinforced concrete bridge column under multidirectional seismic excitation. *Earthquake Engineering and Engineering Vibration* **5:1**, 103-110.